行政院國家科學委員會專題研究計畫 成果報告

無需背景模型之車流分析系統
研究成果報告(精簡版)

計 畫 類 別 ：個別型
計 畫 編 號 ：NSC 99-2221-E-216-049-
執 行 期 間 ：99 年 08 月 01 日至 100 年 07 月 31 日
執 行 單 位 ：中華大學資訊工程學系

計 畫 主 持 人：連振昌
共 同 主 持 人：周智勳
計畫參與人員：碩士班研究生-兼任助理人員：尤文楷
碩士班研究生-兼任助理人員：馬政揚

報 告 附 件 ：出席國際會議研究心得報告及發表論文

處 理 方 式 ：本計畫可公開查詢

中 華 民 國 100 年 10 月 19 日

一、報告內容及參考文獻

部分成果已發表在

[1] **Cheng-Chang Lien**, Ya-Ting Tsai, Ming-Hsiu Tsai, and Lih-Guong Ja, "Vehicle Counting without Background Modeling", 17th International Conference on Multimedia Modeling, MMM 2011, Taipei, Taiwan, January 5-7, Part I, LNCS 6523, pp. 446–456, 2011 **(EI)(LNCS)**

此篇論文並獲推薦刊登於 Journal of Marine Science and Technology(SCI)，報告內容及參考文獻請參閱以下刊登於 MMM 2011 之論文。

Vehicle Counting without Background Modeling

Cheng-Chang Lien[1], Ya-Ting Tsai[1], Ming-Hsiu Tsai[1], and Lih-Guong Jang[2]

[1] Department of Computer Science and Information Engineering,
Chung Hua University, Hsinchu, Taiwan, R.O.C.
Tel.: +886-3-5186404
cclien@chu.edu.tw
[2] Industrial Technology Research Institute, ISTC, Taiwan, ROC

Abstract. In general, the vision-based methods may face the problems of serious illumination variation, shadows, or swaying trees. Here, we propose a novel vehicle detection method without background modeling to overcome the aforementioned problems. First, a modified block-based frame differential method is established to quickly detect the moving targets without the influences of rapid illumination variations. Second, the precise targets' regions are extracted with the dual foregrounds fusion method. Third, a texture-based object segmentation method is proposed to segment each vehicle from the merged foreground image blob and remove the shadows. Fourth, a false foreground filtering method is developed based on the concept of motion entropy to remove the false object regions caused by the swaying trees or moving clouds. Finally, the texture-based target tracking method is proposed to track each detected target and then apply the virtual-loop detector to compute the traffic flow. Experimental results show that our proposed system can work with the computing rate above 20 fps and the average accuracy of vehicle counting can approach 86%.

Keywords: dual foregrounds fusion, texture-based target tracking.

1 Introduction

Recently, many vision-based researches addressed on the vehicle or human detection [1-5] was proposed. In general, the moving objects could be detected by three kinds of methods: motion-based [1], background modeling [2-4], and temporal difference [5] approaches. In the motion-based approaches, the optical flow method [1] utilizes the motion flow segmentation to separate the background and foreground regions. By applying the optical flow method [1], the moving objects can be extracted even in the presence of camera motion. However, the high computation complexity makes the real-time implementation difficult.

For the background modeling methods, the construction and updating of background models [2-4] often is time-consuming. For example, in [2,4], the Gaussian Mixture Model (GMM) is frequently adopted to model the intensity variation for each pixel over a time period and need high computing cost to calculate the GMM parameters. Furthermore, the foreground detection with background modeling method is extremely sensitive to the rapid illumination variation or the dynamic background changing. In [3], the Kalman filter is used to update the background model with less

K.-T. Lee et al. (Eds.): MMM 2011, Part I, LNCS 6523, pp. 446–456, 2011.

computational complexity. But this method can't solve the problem of serious scene change which can make the system unable to update the background model accurately.

The temporal difference method doesn't need to establish the background model instead of subtracting the two adjacent frames and detecting the scene change introduced by the moving objects. The advantage of this method is less susceptible to the scene change, i.e., it has capability to detect the moving objects in dynamic environments. For example, in [5], the temporal difference method is resilient to the dynamic illumination variation, but the regions of the moving objects can't be extracted completely when the objects move slowly.

Here, we propose a novel vehicle detection method without background modeling to overcome the aforementioned problems. First, a modified block-based frame differential method is established to quickly detect the moving targets without the influences of rapid illumination changes. Second, the precise targets' regions are extracted by the dual foregrounds fusion method. Third, a texture-based object segmentation method is proposed to segment each vehicle from the merged foreground image blob and remove the shadows. Fourth, a false foreground filtering method is developed based on the concept of motion entropy to remove the false object regions caused by the swaying trees or moving clouds. Finally, the texture-based target tracking method is proposed to track each detected target and then apply the virtual-loop detector to compute the traffic flow.

The information of vehicle counting may be obtained from several kinds of vision-based sensor [6-10]. However, these methods are difficult to judge whether the vehicle appears in the virtual detector region or not under different lighting conditions. Furthermore, the lack of tracking information will make the vehicle counting inaccurate. Here, a two-line vehicle crossing scheme is applied to count the moving vehicles. The system block diagram is shown in Fig. 1. Our system consists of the following modules: vehicle extraction (foreground detection with dual foregrounds, foreground segmentation, and true object verification), vehicle tracking (Kalman filter tracking), and vehicle counting.

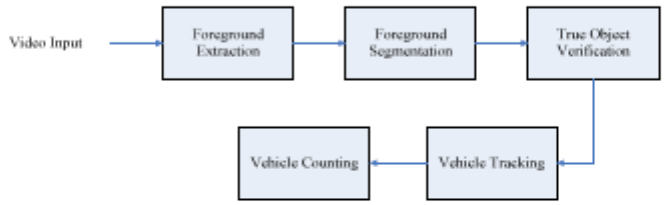

Fig. 1. The block diagram of the traffic flow analysis without background modeling

2 Vehicle Detection without Background Modeling

In general, vehicle detection can't be accurate on the light variation or cluster scenes. In this section, we propose a novel vehicle extraction method without the background modeling to segment the vehicles on the light variation or cluster scenes. Furthermore, to detect the vehicles efficiently and robustly, the motion-based false object filtering method is proposed.

2.1 Adaptive Block-Based Foreground Detection

Traditional pixel-based frame difference method can introduce many fragmented foreground regions because the spatial relationships among neighboring pixels are not considered. Hence, if we detect the moving objects using the frame difference method, both the local and global properties should be considered. Thus, we proposed the block-based foreground detection method to extract more complete foregrounds. First, each frame is divided into the non-overlapped blocks. The block size can be adjusted according to the object size. The foreground detection algorithm is described in the sequel.

1. We transform the RGB color space into the YC_rC_b color space and detect the moving object in Y channel, Cr channel, and Cb channel separately.
2. In each image block, if the number of detected foreground pixels exceeds a specified threshold, then we categorize this block into the foreground block.
3. By fusing the foreground regions detected from Y channel, Cr channel, and Cb channel with the voting rule, we can obtain a more complete object region.

The reason why we adopt the voting method is that Y, Cr, and Cb channels have different property in foreground detection. In Fig. 2-(a), the objects are detected with grayscale's variation in the Y channel; while in Fig. 2-(b)(c), the objects are detected with the color's variations in the Cr and Cb channels. The relationship between grayscale and color information are complementary.

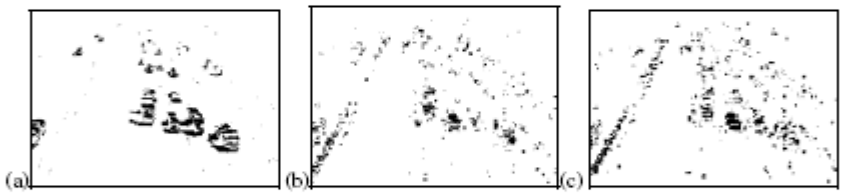

Fig. 2. The difference images for (a) Y channel, (b) Cr channel, and (c) Cb channel

If the region changes in the Y channel but doesn't change in the Cr and Cb channels, then it may be the object shadow. On the contrary, the region changes in the Cr and Cb channels but doesn't change in the Y channel, and then this region may be a noise region. Hence, in our system, the object detection with both the grayscale and color channels is established. The fusing rule is designed by the voting method. We adopted the rule-based method to determine whether the pixel/block belongs to foreground or not.

1. In each image block, if the difference of the Y channel exceed 1.5 times threshold of the Y channel, we classify this block into foreground directly.
2. Otherwise, the object is detected in the Y, Cr, and Cb channels with the rule: $(Y>T_Y)\&\&((Cr>T_{Cr})\|\|(Cb>T_{Cb}))$. If the pixel/block changes in the grayscale and color channels obviously together, then we classify this pixel/block as foreground.

Through the careful observation, we found that the block-based method can extract the more complete foreground than the pixel-based method. When the block size becomes larger, the foreground becomes more complete and the computing time is also faster. However, the condition of wrong connection between different vehicles occurs more frequently.

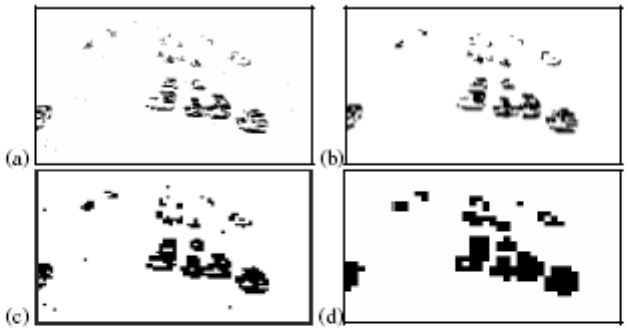

Fig. 3. Block-based foreground extraction. (a) Pixel-based. (b) Block-based (2×2). (c) Block-based (4×4). (d) Block-based (8×8).

Fig. 3 shows the comparison for the block-based and pixel-based method. It is obvious that the moving vehicles extracted with the block-based shown in Fig. 3-(b)(c) are more complete than the pixel-based method shown in Fig. 3-(a). In our experiment, we select the block size as 2×2 to fit the size of moving objects. So far, the block-based foregrounds belong to the short-term foregrounds that will be combined with the long-term foreground to generate a more precise and complete foreground, which will be described in next section.

2.2 Precise Object Region Extraction with the Dual Foregrounds

The traditional frame difference method often generate strong response in the boundary of moving object, but lower response occurs within the region of a moving object shown in Fig. 4-(b). When the object becomes larger, the incomplete object detection will become more serious. To tackle this problem we apply both the characteristic of short-term and long-term foregrounds to make the foreground more complete. The short-term foreground can define precise object boundary and the long-term foreground can extract a more complete object region shown in Fig. 4-(c) with motion history information. The long-term foreground is constructed by accumulating successive short-term foregrounds (In our experiment, the long-term foreground is constructed by accumulating 4 short-term foregrounds). By projecting the short-term foreground onto the long-term foreground, searching the precise object boundary based on the short-term foreground shown in Fig. 4-(f), and preserving all information about short-term and the long-term foregrounds between the boundaries of short-term foreground, we can extract the precise region of a moving vehicle shown in Fig. 4-(g).

2.3 Foreground Segmentation

In the outdoor environment, the serious shadow problem can introduce the inaccurate and false foreground detection shown as the object #4 in Fig.5-(b) and improper merging with neighboring objects shown as the object #2 in Fig. 5-(b). Based on the careful observation, the texture is not obvious in the shadow region illustrated as object #0 in Fig. 5-(b). The texture analysis is then used to eliminate the object shadows. Here, the texture analysis is performed by analyzing the gradient content obtained from the Sobel and Canny operations [11]. By projecting the edge information

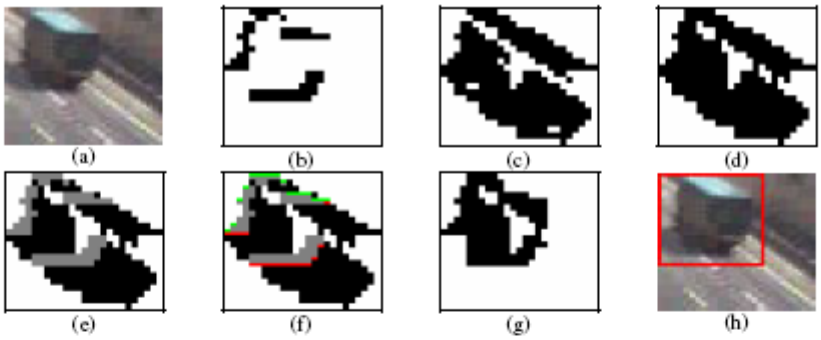

Fig. 4. Procedures for precise object region extraction with dual foregrounds fusion. (a) Original object. (b) Short-term foreground. (c) Long-term foreground. (d) Morphologic operation. (e) Integration of short-term (gray region) and long-term (black region) foregrounds. (f) Fusion with dual foregrounds (Red: upper bound; green: lower bound). (g) Object extraction by fusing the short-term and long-term foregrounds. (h) The bounding box for the extracted object in (g).

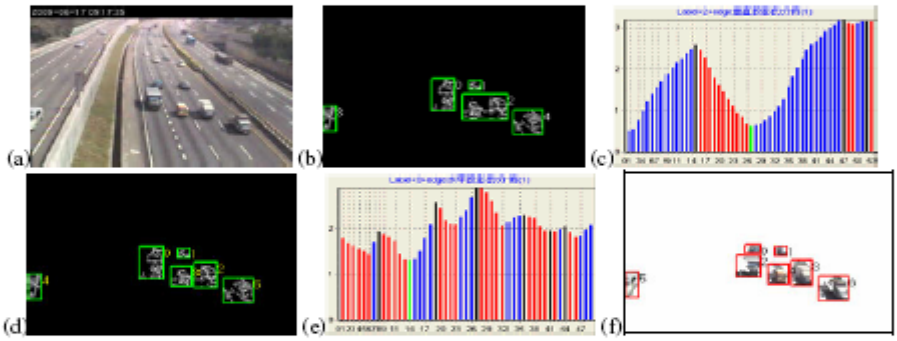

Fig. 5. The procedure of foreground segmentation. (a) Original image. (b) Canny edge detection and object labeling. (c) Edge projection to x-axis of object #2. (d) Object labeling after vertical segmentation. (e) Edge projection to y-axis of object #0. (f) Outcome of texture segmentation.

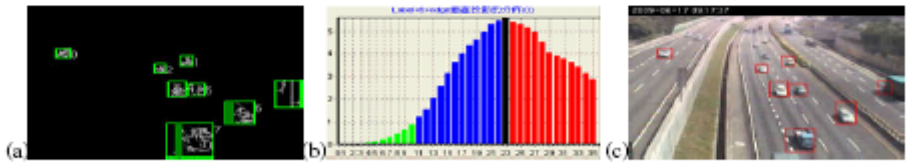

Fig. 6. Removal of the shadow region with the property of texture (a) The texture of foreground. (b) The texture density distribution for the 6th object region. (c) The result of shadow removal.

along horizontal and vertical axes, we can find the proper segmentation position (green bins) using the Ostu's method [12], which are shown in Figures 5-(c) and 5-(e). Once the merged vehicle region is partitioned, each precise vehicle region shown in Fig. 5-(f) is labeled via the labeling algorithm [13].

In general, the distribution of texture density of a moving object is higher than the distribution on its shadow region. Hence, we can utilize the texture densities to separate the moving object and shadow. By removing the boundary vertical regions with small texture density shown in Fig. 6-(b), the shadow region can be separated from the object region shown as the green regions in Fig. 6-(a).

2.5 True Object Verification

For a real moving object, the direction distribution of motion vectors should be consistent, i.e., the motion entropy in the object region will be low. Based on this observation, the value of motion entropy for each detected foreground region can be used to distinguish whether the detected object is a true object or not. First, we apply the three-step block matching method [14] to find the motion vectors for each foreground region and compute the orientation histogram of the motion vectors. Second, we compute the motion entropy for each detected foreground with Eq. (1).

$$E_m = -\sum_{i=1}^{K} p_m^i \log_2 p_m^i \tag{1}$$

where m is object index, i is the index of i-th bin in the orientation histogram, K is the number of total bins in the orientation histogram, and p_m^i is the probability of the i-th bin in the orientation histogram. The motion entropies in these false detected regions are very large and then these false detected regions can be removed with the motion entropy filtering process.

3 Vehicle Tracking

In this study, the texture feature that is not easily influenced by the illumination variation is utilized as the measurement in the target tracking algorithm.

3.1 Kalman Filter

In general, the detected vehicles can be tracked with the methods of Kalman filter or particle filters. With the efficiency consideration, we apply the Kalman filter [17] to track each detected vehicle on the roadway. Each detected vehicle is tracked with the constant-velocity motion model. The state and measurement equations of Kalman filter are defined in Eq. (2).

$$\begin{aligned} x_k &= Ax_{k-1} + w_{k-1} \\ z_k &= Hx_k + v_k \end{aligned} \tag{2}$$

In Eq. (2), x_{k-1} denotes the state at frame k-1, z_k denotes the measurement at frame k, The random variables w_k and v_k represent process and measurement noise. They are assumed to be independent, white, and normal distributed and defined as Eq. (3).

$$\begin{aligned} p(w) &\sim N(0, Q) \\ p(v) &\sim N(0, R) \end{aligned} \tag{3}$$

where, $\boldsymbol{Q}$ denotes the process noise covariance matrix and $\boldsymbol{R}$ denotes the measurement noise covariance matrix. In order to determine whether an observed vehicle belongs to a new incoming vehicle or a previously existed vehicle, we propose an efficient

matching algorithm to calculate the matching distance. For the texture matching, the texture feature can be generated from the canny edge [11] and the distance transform [19]. With the canny edge detection method we can retrieve the rough contours of the detected moving vehicles that is hard to be influenced by the illumination variation and shadow shown in Fig. 7. Then, the distant transform is applied to the canny edge context to retrieve the texture content for the target matching.

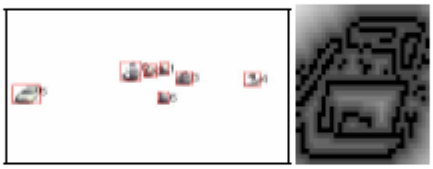

Fig. 7. The extractions of the texture features for each tracked vehicle

Distance transform matching is a technique for finding the matching distance between two different edge features by minimizing shifted template matching defined in Eq. (4).

$$\min_{q,r}\left(\sum_{q=0}^{M-O}\sum_{r=0}^{N-P}\left(\sum_{m=0}^{M}\sum_{n=0}^{N}\left[Tem(m,n)-Ref(o+q,p+r)\right]\right)\right), \tag{4}$$

where *Tem* is the template feature of size $M\times N$ and *Ref* is the reference feature of size $O\times P$. *Tem*(x, y) denotes the pixel value in the template feature and *Ref*(x, y) denotes the pixel value in the reference feature at the position (x, y). If the matching value is less than the specified threshold, we can initialize a new Kalman filter to track or update the Kalman filter with observed vehicle position.

3.2 Vehicle Counting

Here, we set a virtual detecting region on the entire road to monitor whether the vehicles reach the detecting region or not. When a tracked vehicle touches the region, we start to monitor its trajectory within the detecting region. If the vehicle's trajectory

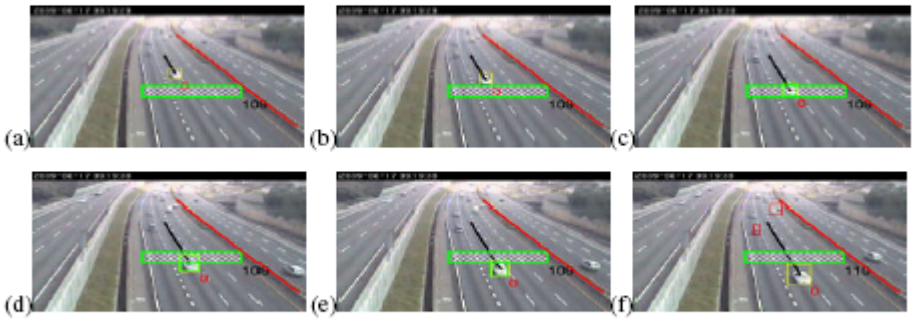

Fig. 8. The procedures of vehicle counting. The tracked vehicle is shown from (a) to (b). The tracked vehicle is driving through the detection region is shown from (c) to (e). (f) The tracked vehicle passes the detection region.

satisfies the following two conditions, then the vehicle is counted. First, the vehicle is detected in the virtual detecting region. Second, the length of the trajectory of a tracked vehicle must larger than a specified length threshold (100 pixels). Some examples of vehicle counting are shown in Fig. 8. In Fig. 8, the red line is used to separate the different directions of traffic flow and the green region is the detection region for counting. The black text represents the current number of passed vehicles.

4 Experimental Results

In this section, the video sequence of PetsD2TeC2 [20] and the real traffic videos captured from the web site of Taiwan Area National Freeway Bureau (http://www.nfreeway.gov.tw) are used as the test videos.

4.1 The Detection of Moving Vehicles

Here we use the PetsD2TeC2 video sequence to evaluate the performance of foreground detection for our method, traditional frame difference method, and the method of background subtracting with Gaussian Mixture Model method.

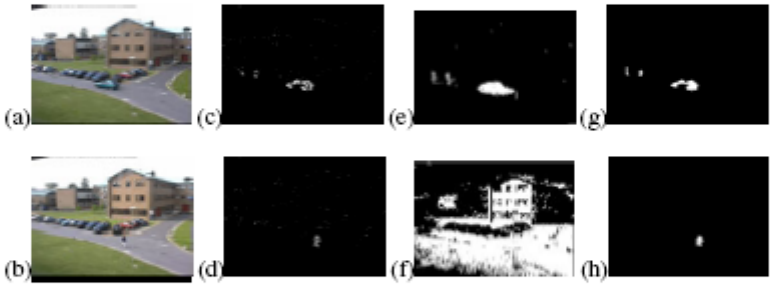

Fig. 9. The examples of foreground detection at frames #1023 and #2517. The original frames are shown from (a) to (b). The foreground detection using the conventional frame difference method is shown from (c) to (d). The foreground detection using the GMM background modeling method is shown from (e) to (f). The foreground detection using our proposed method is show from (g) to (h).

The block size is chosen as 2×2 to fit the size of moving object in our system. The lower bound of object size is set to be 10 blocks for the object detection. The foreground detections in Fig. 9-(c)(d) show the scene adaptability and fragmented region for the frame difference method. The foreground detections in Fig. 9-(e)(f) show the object completeness of the background modeling method [20]. Fig. 9-(f) shows a noisy image that is generated by the inefficient background updating process. The foreground detections in Fig. 9-(g)(h) show the scene adaptability and detection completeness of our proposed method. It is obvious that our method outperforms the other typical methods in terms of scene adaptability and detection completeness. Fig. 10-(a) shows the video sequence of traffic scene on the freeway. Fig. 10-(b) shows that the bounding boxes on the detected vehicles.

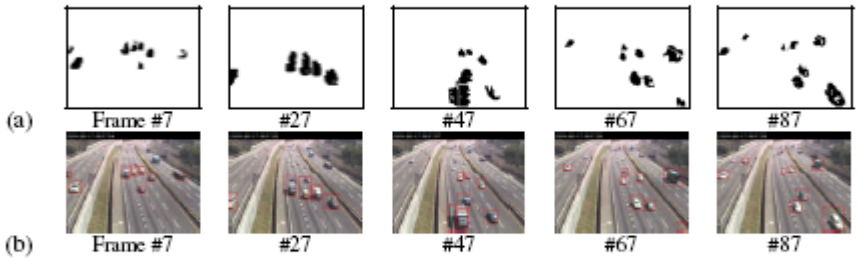

Fig. 10. Moving object detection. (a) A traffic flow scene. (b) The regions of precise moving objects are labeled with red rectangular box.

4.2 Vehicle Tracking and Counting

The vehicle tracking is illustrated in Fig. 11. In Fig. 11-(a), the moving vehicles start to be tracked. Fig. 11-(b)(c) show the correct labeling of the tracked vehicles after the merging and splitting of the two objects. The red rectangular represents the untracked object and the yellow rectangular represent the tracked vehicle. The red number denotes the number of the tracked vehicle.

Fig. 11. Vehicle tracking on crowded vehicle scene

After vehicle tracking, we set a detecting region on the roadway to count the moving vehicles. The detecting region across multiple lanes is used to count vehicles. The performance of vehicle counting is illustrated in Table 1. In the first and second video clips, the density of traffic flow is low. Hence, the performance of the vehicle tracking is satisfied. In the third video clip, the performance is reduced because a few buses introduce the some occlusions and wrong segmentation problems.

Table 1. The accuracy analysis of the vehicle counting

Heading level	1st video clip	2nd video clip	3rd video clip
Actual number	85	88	76
Detected number	90	94	85
False positive	8	9	11
False negative	3	3	2
accuracy	89%	88%	83%

5 Conclusions

In this paper, we propose a novel vehicle detection method without background modeling in which the modified block-based frame differential method, the precise object

region extraction with dual foregrounds, the foreground segmentation, and the true object verification are integrated to develop a scene adaptive vehicle detection system. The texture-based target tracking method is proposed to track each detected target and then apply the virtual-loop detector to analyze the traffic flow. Experimental results show that our proposed system can work in real time with the rate above 20 fps and the accuracy of vehicle counting can approach 86%.

References

[1] Dai, X., Khorram, S.: Performance of Optical Flow Techniques. In: IEEE Computer Society Conference on Computer Vision and Pattern Recognition, pp. 236–242 (1992)

[2] Kamijo, S., Matsushita, Y., Ikeuchi, K., Sakauchi, M.: Traffic Monitoring and Accident Detection at Intersections. IEEE Transactions on Intelligent Transportation Systems 1(2), 703–708 (2000)

[3] Zhou, J., Gao, D., Zhang, D.: Moving Vehicle Detection for Automatic Traffic Monitoring. IEEE Transactions On Vehicular Technology 56(1), 51–59 (2007)

[4] Lien, C.C., Wang, J.C., Jiang, Y.M.: Multi-Mode Target Tracking on a Crowd Scene. In: Proceedings of the Third International Conference on International Information Hiding and Multimedia Signal Processing, vol. 02, pp. 427–430 (2007)

[5] Jain, R., Martin, W., Aggarwal, J.: Segmentation through the Detection of Changes due to Motion. Compute Graph and Image Processing 11, 13–34 (1979)

[6] Wang, K.F., Li, Z.J., Yao, Q.M., Huang, W.L., Wang, F.Y.: An Automated Vehicle Counting System for Traffic Surveillance. In: IEEE International Conference on Vehicular Electronics and Safety (ICVES), pp. 1–6 (2007)

[7] Lei, M., Lefloch, D., Gouton, P., Madani, K.: A Video-based Real-time Vehicle Counting System Using Adaptive Background Method. In: IEEE International Conference on Signal Image Technology and Internet Based Systems, pp. 523–528 (2008)

[8] Qin, B., Zhang, M., Wang, S.: The Research on Vehicle Flow Detection in Complex Scenes. In: IEEE International Symposium on Information Science and Engineering, vol. 1, pp. 154–158 (2008)

[9] Chen, T.H., Lin, Y.F., Chen, T.Y.: Intelligent Vehicle Counting Method Based on Blob Analysis in Traffic Surveillance. In: Second International Conference on Innovative Computing, Information and Control, pp. 238–238 (2007)

[10] Baş, E., Tekalp, A.M., Salman, F.S.: Automatic Vehicle Counting from Video for Traffic Flow Analysis. In: IEEE Intelligent Vehicles Symposium, pp. 392–397 (2007)

[11] Canny, J.: A Computational Approach to Edge Detection. IEEE Transactions on Pattern Analysis and Machine Intelligence 8(6), 679–698 (1986)

[12] Liao, P.S., Chen, T.S., Chung, P.C.: A Fast Algorithm for Multilevel Thresholding. Journal of Information Science and Engineering 17, 713–727 (2001)

[13] Dellepiane, S.G., Fontana, F., Vernazza, G.L.: Nonlinear Image Labeling for Multivalued Segmentation. IEEE Transactions on Image Processing 5(3), 429–446 (1996)

[14] Koga, T., Iinuma, K., Hirano, A., Iijima, Y., Ishiguro, T.: Motion Compensated Interframe Coding for Video Conferencing. In: Proc. Nat. Telecommunication Conf., pp. G5.3.1–G5.3.5 (1981)

[15] Wren, C., Azarbayejani, A., Darrell, T., Pentland, A.: Pfinder: Real-time Tracking of the Human Body. IEEE Transactions on Pattern Analysis and Machine Intelligence 19(7), 780–785 (1997)

二、計畫成果自評

於此計畫所研發之創新技術包括下列數項。第一、我們發展以方塊為基礎之連續畫面差異法以快速偵測移動之車輛，同時不受到強烈的光線變化及大自然中樹的搖晃與移動的雲朵的干擾。第二、經由長短期雙重前景融合分析，我們可以獲得精準且完整之

車輛物體區域。第三、我們提出以紋理為基礎之物體切割技術，來克服從擁擠車群中切割出每一台車輛之區域的問題，也解決傳統以色彩特徵無法準確切割出每一台車輛的缺點。第四、我們提出以物體運動向量之熵值(motion entropy)來過濾樹的搖晃或移動的雲朵所造成的假運動車輛之前景區域。此技術可以應用於道路車流監控及人機手勢互動界面。

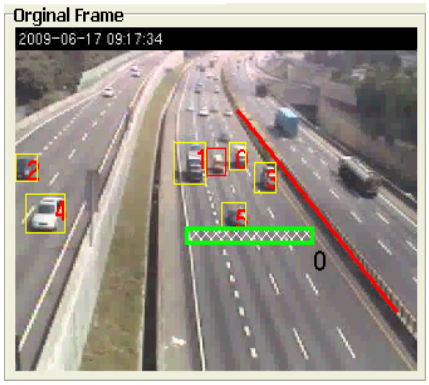

圖一：車流分析系統。

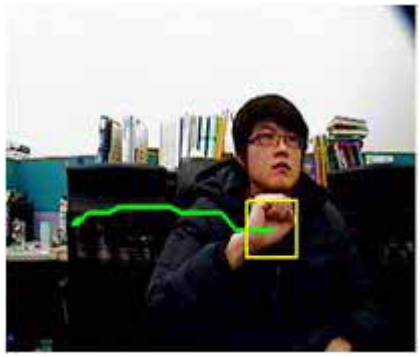

圖二：手勢軌跡人機互動系統。

國科會補助專題研究計畫項下出席國際學術會議報告

日期：100 年 10 月 17 日

計畫編號	NSC 99-2221-E-216-049		
計畫名稱	無需背景模型之車流分析系統		
出國人員 姓名	連振昌	服務機構 及職稱	中華大學資訊工程學系
會議時間	2010 年 10 月 15 日 至 2010 年 10 月 17 日	會議地點	德國 達姆斯塔特
會議名稱	(中文)IEEE 智慧訊息隱藏暨多媒體訊號處理國際會議 (英文) IEEE International Conference on Intelligent Information Hiding and Multimedia Signal Processing 2010 (IIH-MSP 2010) **(EI)**		
發表論文 題目	(中文)利用重取樣性質之快速影像偽造偵測技術 (英文)Fast Forgery Detection with the Intrinsic Resampling Properties		

一、 心得報告

1.1 參加會議經過

這一次參加之會議發表論文一篇，題目為 Fast Forgery Detection with the Intrinsic Resampling Properties。論文主題為提出利用重取樣性質之快速影像偽造偵測技術，如下所列：

Cheng-Chang Lien, Cheng-Lun Shih, and Chih-Hsun Chou, "Fast Forgery Detection with the Intrinsic Resampling Properties," the Sixth International Conference on Intelligent Information Hiding and Multimedia Signal Processing (IIH-MSP-2010), Darmstadt Germany, October 15-17, 2010. **(EI)**

論文摘要如下：

***Abstract*— With the rapid progress of the image editing software, the image forgery can leave no visual clues on the tampered regions and makes us unable to judge the image authenticity. In general, the digital image forgery often utilizes the scaling, rotation or skewing operations in which the resampling and interpolation processes are demanded. By observing the detectable periodic properties introduced from the resampling and interpolation processes, we propose a novel method based on the intrinsic properties of resampling scheme to detect the tampered regions with the pre-calculated resampling weighting table and the periodic properties of prediction error distribution. The experimental results show that the proposed method outperforms the conventional methods in terms of efficiency and accuracy.**

Keywords- image forgery, resampling, forgery detection, intrinsic resampling properties.

會議所報告之 SESSION 為

October 15, 2010			page
Opening		9:00 a.m. – 9:15 a.m.	
Keynote Speech (I)		9:15 a.m. –10:15 a.m.	13
Coffee Break	*Foyer 3.11*	*10:15 a.m. –10:30 a.m.*	
Session A01 – A05		10:30 a.m. –12:30 a.m.	16
Lunch	*Foyer 3.11*	*12:30 a.m. – 2:00 p.m*	
Keynote Speech (II)		2:00 p.m. –3:00 p.m.	13
Coffee Break		*3:00* p.m.–*3:20* p.m.	
Session A06 – A10		3:20 p.m.– 5:20 p.m.	21

October 16, 2010			
Keynote Speech (III)		9:00 a.m. –10:00 a.m.	14
Coffee Break	*Foyer 3.11*	*10:00* a.m. – *10:20* a.m.	
Session B01 – B04		10:20 a.m. – 12:20 a.m.	28
Lunch	*Foyer 3.11*	*12:20* a.m. – *2:00* p.m.	
Keynote Speech (IV)		2:00 p.m. – 3:00 p.m.	14
Coffee Break	*Foyer 3.11*	*3:00* p.m. – *3:20* p.m.	
Session B05– B08		3:20 p.m. – 5:20 p.m.	32
Banquet	*Fraunhofer IGD**	*6:30 p.m. – 8:30 p.m.*	

October 17, 2010			
Keynote Speech (V)		9:00 a.m. – 10:00 a.m.	15
Coffee Break	*Foyer 3.11*	*10:00* a.m. – *10:20* a.m.	
Session C01 – C03, P01		10:20 a.m. – 12:20 a.m.	38, 48
Lunch	*Foyer 3.11*	*12:20* a.m. – *2:00* p.m.	
Session C04 – C06, P02		2:00 p.m. – 4:00 p.m.	41, 48
Coffee Break	*Foyer 3.11*	*4:00* p.m. – *4:20* p.m.	
Session C07 – C09, P03		4:20 p.m. – 6:20 p.m.	44, 48

於會議中也與各國學者交換意見。IIHMSP 會議是由 IEEE 協會主辦，會議所發表之論文也會被 EI 所索引，以增加論文之能見度。這一次 IIHMSP2010 會議之與會圖像記錄如下：

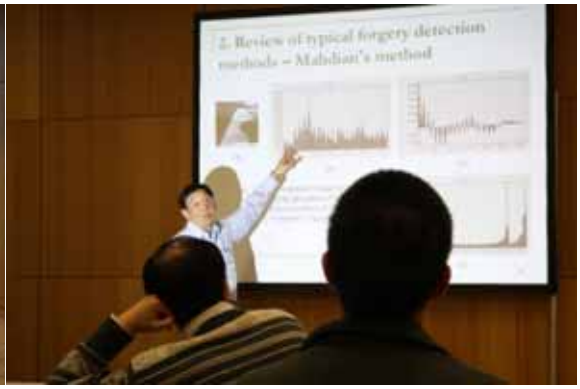

1.2 與會心得

每一次國際會議都會發現許多新技術的發展與應用，以及了解多媒體領域發展的新趨勢。因此研究要與國際接軌，參加國際學術研討會是必要的。

1.3 考察參觀活動(無是項活動者略)

無此項活動

1.4 建議

無

1.5 攜回資料名稱及內容

攜回資料為會議議程及論文光碟片。

二、 論文被接受發表之大會證明文件

The Sixth International Conference on Intelligent Information Hiding and Multimedia Signal Processing
IIH-MSP-2010

October 15-17, 2010, Darmstadt, Germany
http://bit.kuas.edu.tw/~iihmsp10

Dear Prof./Dr./Ms./Mr. **Cheng-Chang Lien**,

Thank you for your submission to the Sixth International Conference on Intelligent Information Hiding and Multimedia Signal Processing (IIH-MSP-2010), to be held on October 15-17, 2010, in Darmstadt, Germany. We are pleased to inform you that your paper

ID No.: **IIH-MSP-2010-IS04-04**
Title: **Fast Forgery Detection with the Intrinsic Resampling Properties**
Author(s): **Cheng-Chang Lien, Cheng-Lun Shih, and Chih-Hsun Chou**

has been accepted for presentation in IIH-MSP-2010. Your paper will be published in the conference proceeding with the Conference Publishing Services of the IEEE CPS. Please do take the comments and suggestions of the reviewers into account in the revision to further improve the quality of your paper. Please refer to http://bit.kuas.edu.tw/~iihmsp10 for further information regarding the conference registration and to the online Author Guide at http://bit.kuas.edu.tw/~iihmsp10 for detailed procedures in the preparation of your camera-ready copy and copyright release form. Both deadlines are July 2nd, 2010.

We are looking forward to meeting you in Darmstadt. Further information on IIH-MSP-2010 can be obtained from the conference web sites:

http://bit.kuas.edu.tw/~iihmsp10

Sincerely Yours,

Xiamu Niu, General Chair
Harbin Institute of Technology, China

Alexander Nouak , Conference executive Chair
Fraunhofer IGD, Germany

Jeng-Shyang Pan, Program Committee Chair
National Kaohsiung University of Applied Sciences, Taiwan

Isao Echizen, Program Committee Chair
National Institute of Informatics, Japan

三、 所發表之論文全文或摘要

2010 Sixth International Conference on Intelligent Information Hiding and Multimedia Signal Processing

Fast Forgery Detection with the Intrinsic Resampling Properties

Cheng-Chang Lien, Cheng-Lun Shih, and Chih-Hsun Chou
Department of Computer Science and Information Engineering
Chung Hua University, Hsinchu, Taiwan, R.O.C.
E-mail: cclien@chu.edu.tw

***Abstract*— With the rapid progress of the image editing software, the image forgery can leave no visual clues on the tampered regions and makes us unable to judge the image authenticity. In general, the digital image forgery often utilizes the scaling, rotation or skewing operations in which the resampling and interpolation processes are demanded. By observing the detectable periodic properties introduced from the resampling and interpolation processes, we propose a novel method based on the intrinsic properties of resampling scheme to detect the tampered regions with the pre-calculated resampling weighting table and the periodic properties of prediction error distribution. The experimental results show that the proposed method outperforms the conventional methods in terms of efficiency and accuracy.**

Keywords- image forgery, resampling, forgery detection, intrinsic resampling properties.

I. INTRODUCTION

In general, the forgery detection and can be further categorized into methods of detecting copy-pasted regions, defocus blur edges, resampling, sensor noise pattern, different lighting conditions and block artifact inconsistency. In [1], the author provided a method to identify the digital forgery regions that are copied and pasted from the same image by applying the method of block matching. However, the matching process can fail if the tampered region is cropped from different images. Zhou et al. [2] proposed a method to identify the digital forgeries by using the edge preserving smoothing filter in which the manual blur edge is discriminated from the defocus blur edge and the erosion operation is applied for detecting the manual blur edge.

Another typical method developed by Popescu [3] detected the digital forgeries by tracing the characteristic of the resampled signals. The major concept of this method is to apply the EM (expectation/maximization) algorithm to acquire the resampling coefficients and then calculate the resampling probability map. Based on the spectral analysis of the probability map, the magnitude peak can be used to identify the forgery patterns. Moreover, Popescu [4] utilized the specific interpolation coefficients of color filter array for each brand of digital camera to identify the digital forgery. Kirchner [5] proposed a more efficient method by directly applying the converged resampling coefficients to detect the tampered regions. As same as tracing the periodic characteristic of the resampled signals, Prasad [6] and Mahdian [7-8] proposed their method to extract the periodical property of the resampled signals based on analyzing the periodic characteristic of the covariance of the second order derivatives.

Generally, each kind of digital forgery detection method can solve only one kind of forgery pattern. In this study, we only address on the detection of resampling forgery. Two related researches addressed on the detection of resampling forgery are the methods proposed by Popescu [3] and Mahdian [7]. However, there exist two major drawbacks in the above-mentioned algorithms. For the Popescu's method [3], high computation cost in the iterative computing procedure is required. It takes almost 5 minutes to generate the probability map for the image with resolution 512×512 pixels. For the method proposed by Mahdian [7], we found that the derivative kernel used in [7] will destroy the periodicity of the correlation function at the high texture regions. Hence, in this study, we try to investigate and analyze the intrinsic properties of resampling scheme and develop a new more efficient algorithm based on the intrinsic properties of resampling.

II. RELATED WORKS

A. The Popescu's Method

A well known forgery detection method proposed by Popescu [3] assume that the interpolated samples are the linear combination of their neighboring pixels and try to train a set of resampling coefficients to estimate the probability map. In this method, a digital sample can be categorized into two models: M_1 and M_2. M_1 denotes the model that the sample is correlated to their neighbors; while M_2 denotes that the sample isn't correlated to its neighbors. The resampling coefficients can be acquired by the EM algorithm. In the E-step, the probability for M_1 model for every sample is calculated. In the M-step, the specific correlation coefficients are estimated and updated continuously. After applying the Popescu's method to the image, we can obtain a probability map. The peak ratio of frequency response of the probability map can be used to identify the digital forgery.

B. The Mahdian's Method

Another method proposed by Mahdian and Saic [7] demonstrates that the interpolation operation can exhibit periodicity in their derivative distributions. To emphasize the periodical property, they employ the radon transformation to project the derivatives along a certain orientation. After projecting all the derivatives to one direction and forming 1-D projection vectors, the

978-0-7695-4222-5/10 $26.00 © 2010 IEEE
DOI 10.1109/IIHMSP.2010.65

autocovariance function can be used to emphasize the periodicity and defined as:

$$R_{\rho_\theta}(k) = \sum_i (\rho_\theta(i+k) - \overline{\rho_\theta})(\rho_\theta(i) - \overline{\rho_\theta}) \quad (1)$$

Then, the Fourier transformation of $R_{\rho\theta}$ are also computed to identify the periodic peaks which can identify the digital forgery.

III. Forgery Detection using the Resampling Intrinsic Properties

There exist two major drawbacks in the above-mentioned algorithms. For the Popescu's method [3], high computation cost in the iterative computing procedure is required. It takes almost 5 minutes to generate the probability map for a image with resolution 512×512 pixels. For the method proposed by Mahdian [7], we found that the derivative kernel used in [7] can reduce the periodicity of the correlation function at the high texture region. Hence, in this study we try to investigate and analyze the intrinsic properties of resampling process and develop a new more efficient algorithm.

A. *Intrinsic Properties of Resampled Signal*

In this section, we firstly introduce the procedures of general resampling process. The up-sampling process is illustrated in Fig. 1-(a) and the original values are denoted as red bars. Fig. 1-(b) shows that interpolation operation fills the empty points with the linear combination of the adjacent signals' values which are denoted as yellow bars. Finally, the samples selected for decimation process which are denoted as blue bars are shown in Fig. 1-(c). Through the observation of the resampling process, it gives us an important clue to design a new forgery detection algorithm, which is the original value will appear periodically in the resampling process.

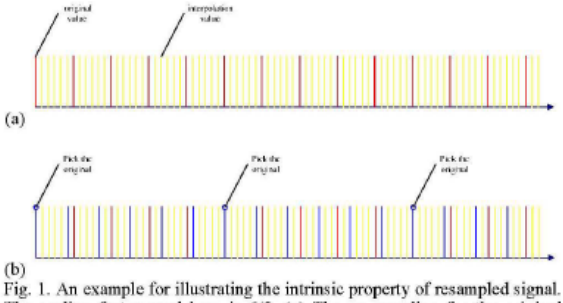

Fig. 1. An example for illustrating the intrinsic property of resampled signal. The scaling factor used here is 6/5. (a) The up-sampling for the original values (red bars). Linear interpolation is denoted as yellow bars. (b) Down sampling of signal in (a). The resampled signal is denoted as blue bars. The blue bars labeled the white node denote that the original values are chosen.

B. *Periodicity of the Prediction Error*

Every resampled value denoted as blue bar in Fig. 3 can be approximated by the linear combinations of the adjacent original values denoted as red bar with different weights according to their positions, i.e., the weighting in the linear interpolation algorithm is propositional to the distance to their neighbors. Here, we pre-calculate the weighing table for each resampling rates. If the resampling rate is known, then the original values can be approximated by the linear combination of the interpolated values. Based on the periodical property of the original values selected from resampling, some of the approximated values would exactly overlap the original values in resampled signals shown as the green bar in Fig. 1-(b). Ideally, the error between the predicted value and the resampled value would be very small at the position where the original value is resampled (the green bar in Fig. 2). Moreover, the variation of the prediction error will distribute periodically. The weighting table $W_T[i]$, $i = 1, 2, \ldots, N$, should be calculated in advance for each resampling rate. The prediction process is described in Fig. 2.

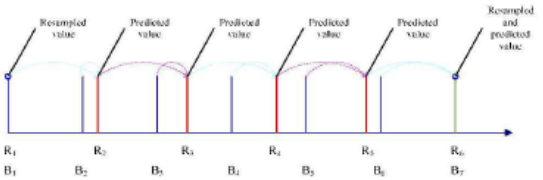

Fig. 2. The values (red bar) could be predicted by the resampled values (blue bar). After a certain periodical time interval, the predicted value will overlap the original value denoted as green bar.

In Fig. 2, the interpolated values can be computed as:

$$B_1 = R_{i-1} \times WT_L[i-1] + R_i \times WT_R[i-1] \quad (2)$$

Then, the predicted resampling values can be computed as:

$$pre_1 = R_2 = \frac{B_2 - R_1 * WT_L[i]}{WT_R[i]}$$

$$pre_2 = R_3 = \frac{B_3 - pre_1 * WT_L[i]}{WT_R[i]}$$

$$\ldots$$

$$pre_m = R_N = \frac{B_N - pre_{m-1} * WT_L[i]}{WT_R[i]} = B_{N+1} \quad (3)$$

Finally, the prediction error within the certain sliding window can be computed as:

$$\text{Prediction error} = |B_{N+1} - pre_m|. \quad (4)$$

For the case of resampling rate 120%, the difference between pre_5 and B_7 will be very small. When the sliding window for calculating the sample prediction is moving (shown in Fig. 3), the prediction error will increase and then decrease to the minimum value until the sliding window moves to the next periodical position (B_{14}, B_{21}…). Such a periodical property makes the sequence of prediction error distribute periodically shown in Fig. 4-(d). In order to enhance this property, the projection operation is also performed for every row and column (two directions are considered separately) before we utilize the frequency analysis to detect the forgery patterns (peaks in frequency response). If the test samples are not resampled or the wrong weighting table is selected, the distribution of prediction error would be irregular.

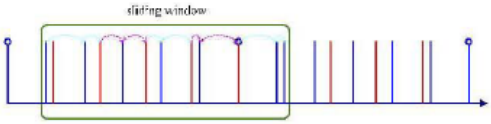

Fig. 3. The sliding window for calculating the sample prediction using the pre-calculated weighting table.

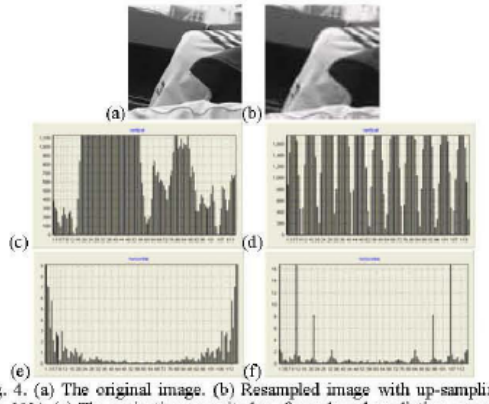

Fig. 4. (a) The original image. (b) Resampled image with up-sampling rate 10%. (c) The projection magnitudes of row-based prediction error of (a). (d) The projection magnitudes of row-based prediction error of (b). (e) The frequency response of (c). (f) The frequency response (d).

To develop an automatic forgery detection method, there are two main criteria should be considered. The first one is the position where the peak occurs and the second one is the peak ratio. According to the different weighting tables (different resampling rate) for the forgery detection and the specific periodical property for each resampling rate, the expected position where the peak occurs could be forecasted. Then, we can match the peak position to the forecasted position where the specific resampling rate generates for identifying the existence of digital forgery. If the ratio is larger than a specified threshold, we can identify that existence of digital forgery. To detect the tampered region, the image is scanned from left-top to right-bottom with different block sizes. In each block, the proposed method is applied to detect the tampered regions.

IV. Experimental Results

The experimental database is constructed with 160 gray level images with resolution 512×512 and each image is partial tampered in BMP format. The image tampering is based on the resampling process with the different bi-linear sampling rates: 105%, 110%, 120% and 125%. The forgery detections are performed by scanning the image with the block size of 128 × 128 pixels. Before analyzing the accuracy of forgery detection, we firstly describe the detection rules for the Popescu's [3], Mahdian's [7], and our methods. Here, the forgery detection of Popescu's and Mahdian's methods is determined by evaluating whether the ratio of peak-to-average frequency response is larger than a predefined threshold value or not. The ratio of peak-to-average frequency response is defined as:

$$R_{Popescu} = R_{Mahdian} = \frac{magnitude_{maximum}}{magnitude_{average}}$$

For our method, the forgery detection is determined by evaluating whether the ratio of forecasted peak-to-average frequency response is larger than a predefined threshold value or not. The ratio of forecasted peak-to-average frequency response is defined as:

$$R_{our} = \frac{magnitude_{forecastedposition}}{magnitude_{average}}$$

The resampled image with rate 120% shown in Fig. 5-(a) is used as the tampered image for analyzing the detection accuracy for the three methods. Fig. 5-(b) shows the probability map produced by the Popescu's method and Fig. 5-(c) shows the frequency response of the probability map. Fig. 6-(a) shows the radon transformation of the derivative along horizontal direction. Fig. 6-(b) shows the auto-covariance of Fig. 6-(a) and Fig. 6-(c) shows the frequency response of the auto-covariance values. The prediction error generated by our method is shown in Fig. 7-(a). Fig. 7-(b) presents the frequency response of the prediction error. An obvious drawback of the Mahdian's method is that the weak periodical patterns occur at the high texture regions shown in Fig. 5-(b). The accuracy of forgery detections for different resampling rates is analyzed in Table 1.

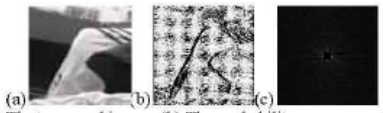

Fig. 5. (a) The tampered image. (b) The probability map generated by the Popescu's method. (c) The frequency response of (b).

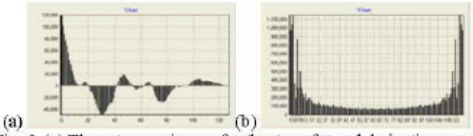

Fig. 6. (a) The autocovariance of radon transformed derivatice maps obtained by the Mahdian's method. (b) The frequency response of (a).

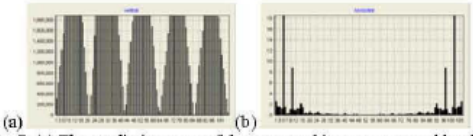

Fig. 7. (a) The prediction error of the tampered image generated by the proposed method for Fig 5-(a). (b) The frequency response of (a).

The ROC curves with different up-sampling rate for Popescu's, Mahdian's and our methods are shown in Fig. 8. In this Figure, the detection accuracy of Popescu's method is highest, and the detection accuracy of our method is close to the Popescu's curve. However, our method is the fastest one that will be mentioned later. The detection accuracy of Mahdian's method is the lowest because the detection accuracy is affected by the high texture regions. In addition,

we compare the efficiency among Popescu's [3], Mahdian's [7] and our methods with the PC of 1.8 GHz. The efficiency analysis is shown in Fig. 11. Here, we perform the efficiency analysis from block size 64×64 to 512×512 and assume there are 21 weighting tables for 21 resampling rates used in [3]. It's worthy to conclude that detection accuracy and efficiency of our method can approach both of the benefits of Popescu's and Mahdian's methods.

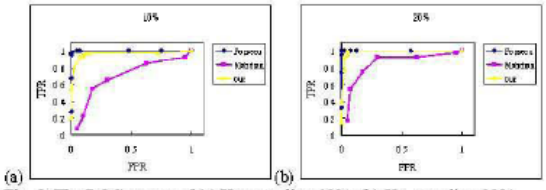

(a) (b)

Fig. 8. The ROC curves of (a) Up-sampling 10%. (b) Up-sampling 20%.

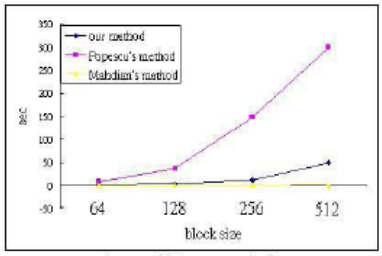

Fig. 9. Efficiency analysis.

Fig. 10 shows the detection results of the proposed method for different resampling rates with two block sizes. Fig. 10-(a) and Fig. 10-(b) show the detection result with 64×64 and 128×128 block sizes. Here, we observe that the detection accuracy for the smaller block size is lower than the accuracy with larger block size because more periodical patterns can be collected in larger blocks.

V. Conclusion

In this paper, we propose a novel method based on the intrinsic properties of resampling scheme to detect the forgery regions with the pre-calculated resampling weighting tables. In Popescu's method, high accuracy can be obtained with high computation cost. On the contrary, in Mahdian's method, the detecting accuracy can be affected on the high texture regions. The detection accuracy and efficiency of our method can approach both of the benefits of Popescu's and Mahdian's methods. The detection accuracy of our method is about 95% and the time for detecting a 512×512 image needs only 50 seconds.

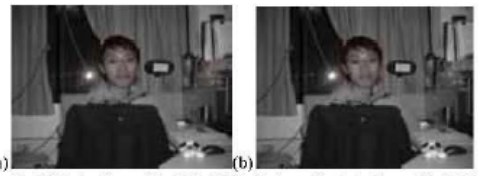

(a) (b)

Fig. 10. (a) Detection with 64×64 block size. (b) Detection with 128×128 block size.

References

[1] J. Fridrich, D. Soukal and J. Lukáš, "Detection of copy-move forgery in digital images," Proceedings of the Digital Forensic Res. Workshop, 2003.

[2] L. Zhou, D. Wang, Y. Guo and J. Zhang, "Blue detection of digital forgery using mathematical morphology," Technical report, KES AMSTA, pp. 990-998, 2007.

[3] A. C. Popescu and H. Farid, "Exposing digital forgeries by detecting traces of resampling," IEEE Transactions on Signal Processing, vol. 53, pp. 758–767, 2005.

[4] A. C. Popescu and H. Farid, "Exposing digital forgeries in color filter array interpolated images," IEEE Transactions on Signal Processing, vol. 53, pp. 3948–3959, 2005.

[5] M. Kirchner, "Fast and reliable resampling detection by spectral analysis of fixed linear predictor residue," MM&Sec'08, Proceedings of the Multimedia and Security Workshop, pp. 11-20, 2008.

[6] S. Prasad and K. Ramakrishnan, "On resampling detection and its application to detect image tampering," Proceedings of the 2006 IEEE International Conference on Multimedia and EXPO, pp. 1325–1328, 2006.

[7] B. Mahdian and S. Saic, "Blind authentication using periodic properties of interpolation," IEEE Transactions on Information Forensics and Security, in press, 2008.

[8] B. Mahdian and S. Saic, "Detection of resampling supplemented with noise inconsistencies analysis for image forensics," International Conference on Computational Sciences and Its Applications, pp. 546-556, 2008.

TABLE 1. THE ACCURACY ANALYSIS FOR THE METHODS OF OUR, POPESCU'S AND MAHDIAN'S WITH 40 RESAMPLED IMAGES FOR DIFFERENT RATES.

	Popescu's method				*Our method*				*Mahdian's method*			
Up-sampling	5%	10%	20%	25%	5%	10%	20%	25%	5%	10%	20%	25%
Positive	40	40	40	40	40	40	40	40	40	40	40	40
Negative	40	40	40	40	40	40	40	40	40	40	40	40
True positive	40	39	40	40	38	39	40	40	21	22	37	37
True negative	40	40	40	40	35	37	38	38	25	33	28	30
Accuracy	100%	98.7%	100%	100%	91.2%	95%	97.5%	97.5%	57.5%	68.7%	81.2%	83.7%

國科會補助計畫衍生研發成果推廣資料表

日期:2011/10/04

國科會補助計畫	計畫名稱: 無需背景模型之車流分析系統
	計畫主持人: 連振昌
	計畫編號: 99-2221-E-216-049- 學門領域: 影像處理

無研發成果推廣資料

99 年度專題研究計畫研究成果彙整表

計畫主持人：連振昌	計畫編號：99-2221-E-216-049-
計畫名稱：無需背景模型之車流分析系統	

成果項目			量化			單位	備註（質化說明：如數個計畫共同成果、成果列為該期刊之封面故事...等）
			實際已達成數（被接受或已發表）	預期總達成數(含實際已達成數)	本計畫實際貢獻百分比		
國內	論文著作	期刊論文	0	0	100%	篇	
		研究報告/技術報告	0	0	100%		
		研討會論文	0	0	100%		
		專書	0	0	100%		
	專利	申請中件數	0	0	100%	件	
		已獲得件數	0	0	100%		
	技術移轉	件數	0	0	100%	件	
		權利金	0	0	100%	千元	
	參與計畫人力（本國籍）	碩士生	0	0	100%	人次	
		博士生	0	0	100%		
		博士後研究員	0	0	100%		
		專任助理	0	0	100%		
國外	論文著作	期刊論文	1	1	100%	篇	
		研究報告/技術報告	0	0	100%		
		研討會論文	1	1	100%		
		專書	0	0	100%	章/本	
	專利	申請中件數	0	0	100%	件	
		已獲得件數	0	0	100%		
	技術移轉	件數	0	0	100%	件	
		權利金	0	0	100%	千元	
	參與計畫人力（外國籍）	碩士生	2	2	100%	人次	
		博士生	0	0	100%		
		博士後研究員	0	0	100%		
		專任助理	0	0	100%		

其他成果 (無法以量化表達之成果如辦理學術活動、獲得獎項、重要國際合作、研究成果國際影響力及其他協助產業技術發展之具體效益事項等，請以文字敘述填列。)	1. 此研究部分成果已發表在 17th International Conference on Multimedia Modeling, MMM 2011, 並刊登於 Part I, LNCS 6523, pp. 446 – 456, 2011 (EI)(LNCS)。 2. 此篇論文並獲推薦刊登於 Journal of Marine Science and Technology(SCI)。 3. 此技術與中強光電及瑞昱半導體洽談技術移轉。

	成果項目	量化	名稱或內容性質簡述
科教處計畫加填項目	測驗工具(含質性與量性)	0	
	課程/模組	0	
	電腦及網路系統或工具	0	
	教材	0	
	舉辦之活動/競賽	0	
	研討會/工作坊	0	
	電子報、網站	0	
	計畫成果推廣之參與（閱聽）人數	0	

國科會補助專題研究計畫成果報告自評表

請就研究內容與原計畫相符程度、達成預期目標情況、研究成果之學術或應用價值（簡要敘述成果所代表之意義、價值、影響或進一步發展之可能性）、是否適合在學術期刊發表或申請專利、主要發現或其他有關價值等，作一綜合評估。

1. 請就研究內容與原計畫相符程度、達成預期目標情況作一綜合評估

■達成目標

□未達成目標（請說明，以 100 字為限）

□實驗失敗

□因故實驗中斷

□其他原因

說明：

2. 研究成果在學術期刊發表或申請專利等情形：

論文：■已發表 □未發表之文稿 □撰寫中 □無

專利：□已獲得 □申請中 ■無

技轉：□已技轉 □洽談中 ■無

其他：(以 100 字為限)

Cheng-Chang Lien, Ya-Ting Tsai, Ming-Hsiu Tsai, and Lih-Guong Ja, ’Vehicle Counting without Background Modeling’, 17th International Conference on Multimedia Modeling, MMM 2011, Taipei, Taiwan, January 5-7, Part I, LNCS 6523, pp. 446－456, 2011 (EI)(LNCS)

3. 請依學術成就、技術創新、社會影響等方面，評估研究成果之學術或應用價值（簡要敘述成果所代表之意義、價值、影響或進一步發展之可能性）（以 500 字為限）

對於車流分析檢測交通流量或交通堵塞,在智慧型運輸系統(intelligent transportation systems，ITS）是重要的研究問題。然而，以視覺為基礎之車流偵測技術通常會面臨到幾個問題。首先是強烈的戶外光線變化會影響車輛偵測的正確性。再者是大自然中樹的搖晃或移動的雲朵也會造成非車輛物體之偵測而造成假物體的干擾。因此，我們研發一項無需背景模型之車流分析系統以克服上述所提到的問題。於此計畫所研發之新系統裡包含數項新的技術研發。第一、我們發展改良之以方塊為基礎之連續畫面差異法以快速偵測移動之車輛，同時不受到強烈的光線變化及大自然中樹的搖晃與移動的雲朵的干擾。第二、經由長短期雙重之前景融合(fusion of short-term and long term backgrounds)分析，我們可以獲得精準且完整之車輛物體區域。第三、我們提出以紋理為基礎之物體切割技術來克服從擁擠車群中切割出每一台車輛之區域，也解決傳統以色彩特徵無法準確切割出每一台車輛的缺點。第四、我們提出以物體運動向量之熵值(motion entropy)來過濾樹的搖晃或移動的雲朵所造成的假運動車輛之前景區域。最後，結合上述所研發之技術，於本計畫裡我們會發展出以紋理模型做為車輛追蹤之新技術，並利用此技術分析車流及偵測相關異常事件。從實驗的結果發現，本研究能在一個光線劇烈變化的環境下正確的作車流分析，並且每秒約可處理 20 張 frame。目前此技術可以應用於道路車流監控及人機手勢互動界面。